

Synthesis and surface modification of chitosan built nanohydrogel with antiviral and antimicrobial agent for controlled drug delivery

Faheem Ullah¹ , Fatima Javed² , Abdul Naeem Khan³ , Muhammad Helmi Abdul Kudus¹ , Nargis Jamila² , Aaliya Minhaz² , Hazizan Md. Akil^{1,*} 

¹School of Materials and Mineral Resources Engineering, Universiti Sains Malaysia, Seri Ampangan, 14300 Nibong Tebal, Pulau Penang, Malaysia

²Department of Chemistry, Shaheed Benazir Bhutto Women University, Peshawar 25000, Khyber Pakhtunkhwa, Pakistan

³National; Centre of Excellence in Physical Chemistry, University of Peshawar, 25120, Pakistan

*corresponding author e-mail address: hazizan@usm.my | Scopus ID [7102836574](https://orcid.org/0000-0002-7102-8365)

ABSTRACT

As hydrophobic drug carriers, chitosan (CS) and Starch (SR) were copolymerized as biodegradable nanohydrogel and were functionalized with phthalic-anhydride and hexamethylenetetramine via 1-ethyl-3-(3-dimethylaminopropyl) carbodiimide catalyzed coupling, respectively. The structure, morphology, physicochemical and drug loading performance of native and functionalized hydrogel were investigated by using several characterization techniques. With the successive functionalization the significant properties like porosity increases and crosslinking density decreases due to the formation of hydrophilic contacts with aqueous solutions. The FESEM analysis revealed the hydrogel matrices with uniform particle size, porosity and deep pores with high internal surface area for extreme swelling and interacting with the drug and biomolecules for efficient drug administration. The effect of induced functionalities on the physicochemical performance and release of hydrophobic- anionic model drug (Bromocresol green) were studied at physiological conditions. The drug release capability of the synthesized nanohydrogel was increased from 65% to 80% and 85% by successive functionalization. The drug administration in selective hydrogel was not significant, presumably due to stronger H-bonding and entanglement within the system which was finely tuned by the induced hydrophilic, flexible and biocompatible functionalities in term of extended interfaces for the drug solutions. The physicochemical and electrokinetic performances suggested the selective hydrogel as promising carriers for the hydrophobic- anionic drugs at physiological conditions.

Keywords: *Nanohydrogel; surface modification; antiviral and antimicrobial; in-vitro drug release.;*

1. INTRODUCTION

The biomaterials in the form of hydrogel matrices, with bioactive interfaces and developed functionalities, serves best to reflect the theme of controlled drug delivery. Further, how to induce the sensitivity (like antiviral, antimicrobial, amphiphilic and drug administration capabilities) into selective hydrogel network (SHN) to deliver and hit the targeted sites at physiological conditions is still unanswerable [1, 2]. Therefore, the hydrogel and their surface modification by desired functionalities with understandable chemistry, synthetic strategies, low-temperature treatment, chemical control, better compatibility, high surface area (for drug administration) and versatile external surfaces (available for functionalization by desired biomolecules and ligands) has no matching if explored properly.

A three dimensional network of polymers made of natural or synthetic materials possessing a high degree of flexibility due to large water content is called hydrogel. Under physiological conditions, they are able to retain a large amount of water or biological fluids and are characterized by a soft rubbery consistency similar to living tissues, making them an ideal substance for a variety of applications [3, 4]. Hydrogel with characteristic properties such as desired functionality, reversibility, stabilizability and biocompatibility meet both material and biological requirements to treat or replace tissues, or the function of living tissues, as well as to interact with the

biological system and different hydrophilic and hydrophobic drugs [5, 6].

Biomaterials are ideal to fabricate a different hydrogel system for clinical practice and experimental medicine due to: ease of availability from renewable resources (like plants, animals, algae, and microbes), the diverse structures, functionalities, desirable properties and pendant groups that cannot be mimicked by synthetic materials to work at physiological conditions [7]. Thus, the most promising, biocompatible and biodegradable chitosan and starch were considered as the starting materials to fabricate chemically- crosslinked hydrogel networks. The biodegradable polymer such as chitosan, a pH-dependent polycation, where the relevant chains are able to interact with oppositely charged molecules through electrostatic interactions, is highly recommended for drug delivery, wound dressing, tissue engineering and biotechnology applications. Chitosan is known to protect the drug from hostile and antagonistic environment. Chitosan is only soluble in water at a pH that is below 6.5 (\approx pKa value of chitosan), where the protonation of the amine group will help to create positive charges and the resultant repulsion of the group will assist in solubilization and swelling. Another important aspect of selecting chitosan for the proposed system is its efficient removal through renal filtration and enzymatic degradation [8-11]. Similarly, starch is known as the most common polymeric carbohydrate. In pharmaceutical industry starch is used as safe

tablet disintegrant, binder and long-term stabilizing agent as excipient (a substance formulated alongside the active ingredient of a medication, for the purpose of long-term stabilization. Starch is introduced as new material to produce interpenetrating hydrogel networks. In hydrolyzed form starch can be employed as monomer/ oligomer [12]. It can also be grafted to produce functional polymers. Therefore, this combination of chitosan and starch is a clear sign to produced safe, biocompatible and functional hydrogel to act as controlled drug delivery system at physiological conditions.

The functionalization approached aim to add the antiviral and antimicrobial properties to the selective hydrogel for efficient and safe drug delivery applications. In addition the selective functional moieties mean to act as chelating agents. Chelation therapy is the use of chelating agents to detoxify a patient's body of poisonous metal agents, such as mercury, arsenic and lead by converting them to a chemically inert form that can be excreted without further interaction with the body [13]. The functionalization moieties were selected as phthalic-anhydride (PA) and hexamethylenetetramine (HA) respectively. PA is considered as versatile intermediate in organic chemistry and used in the pharmaceutical industry as long term coating excipient characterized with antiviral properties. Further, hexamethylenetetramine (HA) which is a heterocyclic organic compound, soluble in water only at acidic conditions, having a cage like structure used as preservative and to treat urinary tract infection. It decomposes in acidic conditions to produce formaldehyde, which is highly bactericidal as bacteria do not

develop resistance to formaldehyde. The art and fundamental of selective functional moieties in carbodiimide cross coupling are shown in **Figure 1** as:

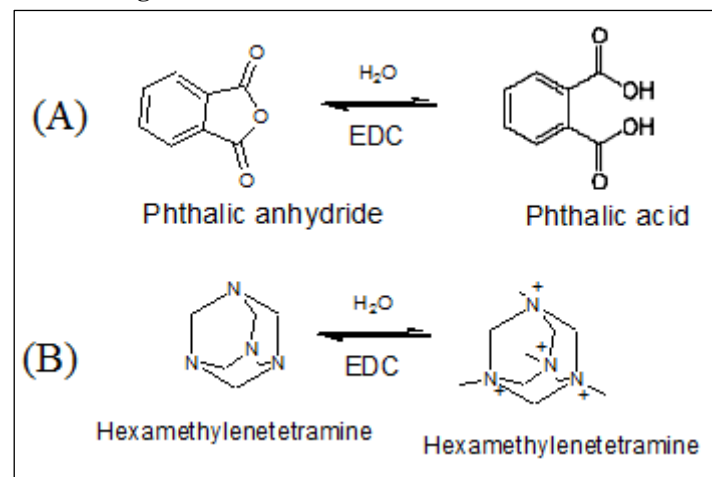


Figure 1. Surface modification of chitosan built hydrogel with bioactive, hydrophilic, antiviral (A) and antifungal (B) ligands for efficient drug delivery.

The objective of this work is to examine the formation of CS-co-SR nanohydrogel and their respective functionalization with hydrophilic functionalities as phthalic anhydride (PA) and hexamethylenetetramine (HA) via 1-ethyl-3-(3-dimethylaminopropyl) carbodiimide (EDC) with induced antiviral and antimicrobial properties in addition to producing hydrophilic contacts for extended interactions of functional hydrogel with the drug solutions for controlled drug delivery applications.

2. MATERIALS AND METHODS

2.1. Materials.

Medium-molecular-weight chitosan ($M_w = 95,000$ g/mol, degree of deacetylation = 94%, viscosity of 1% solution in 1% acetic acid = 715 cP), starch ($M_w = 750.64$ g/mol, viscosity of 1% solution in 1H₂O = 425.75 cP), crosslinker- carbodhyrize (CH), initiator- Ammonium persulphate (APS) and 1-ethyl-3-(3-dimethylaminopropyl) carbodiimide (EDC), phthalic-anhydride(PA) and hexaethylenteteramine (HA) were purchased from Sigma Aldrich (St. Louis, MO, USA). All chemicals used were of analytical grade. All the buffer solutions were used as received without purification. All the buffer solutions were used as received without further purification. Deionized distilled water (DDH₂O) followed by filtration through a membrane filter with pore size ≈ 0.45 microns (to remove any entrapped dust particles) was used for solution preparation, polymerization, dialysis and analysis steps.

2.2. Synthesis and surface modification/ functionalization of chitosan built nanohydrogel.

As per literature, chitosan built hydrogel have been synthesized from several methods [14-18]. In this study, C1CS-co-SR nanohydrogels were prepared by free radical copolymerization method as reported earlier [19]. By using the thermal initiator system, the hydrogels were prepared at 72 °C as sketched in **Figure 2**. Briefly, 650 mg of Chitosan was dissolved in 85 mL of DDH₂O containing 1% of acetic acid for 20 h at room temperature. The temperature of the solution was then gently raised at the speed of 2 °C /min until the required temperature was achieved. 550 mg of dissolved starch along with a 0.5 M aqueous

solution of the thermal initiator (APS) was added to the reaction mixture after one hour of achieving the required temperature. Exactly after 30 minutes of polymerization, aqueous solution of 0.5 M crosslinker (carbodhyrize) was added to the system under constant stirring and N₂ purging. After some time the system became progressively thicker and was observed until it could not be stirred. The resultant hydrogel was then purified by centrifugation, decantation followed by frequently washing with DDH₂O. Finally the hydrogel was purified at room temperature by dialysis for 07 days in membrane tubing (Spectrum laboratories, Inc., Rancho Dominguez, CA, USA; MW cutoff 12,000–14,000). The product was dewatered using ethanol for 02 h, cut into small pieces, grinded and again washed with ethanol and then filtered. The particles were dried in an oven at 70 °C for 48 h. The particles were stored in absence of heat, light and moisture after fine grinding. The feed composition is shown in **Table 1**. The functionalization of CS-co-SR hydrogel by the respective ligand known as phthalic-anhydride (PA) and hexaethylenteteramine (PA) was carried out as follows. 0.125 g of PA and 0.125 g of 1-Ethyl-3-(3-dimethylaminopropyl) carbodiimide known as EDC was dissolved in 70 ml DDH₂O with continuously stirring for 10 h at room temperature. The solution was then placed in an ice bath followed by the addition of 100 mL of dialyzed hydrogel under continuous stirring for 5 h to functionalize the hydrogel via EDC catalyzed coupling of PA to replace -OH groups in CS units followed by dialysis for one week. A similar scheme was followed for the functionalization of hydrogel by HA, via EDC catalyzed coupling, to replace OH groups in CS units. Finally the hydrogel

products were dried in vacuum oven at 70 °C to gain a stable mass

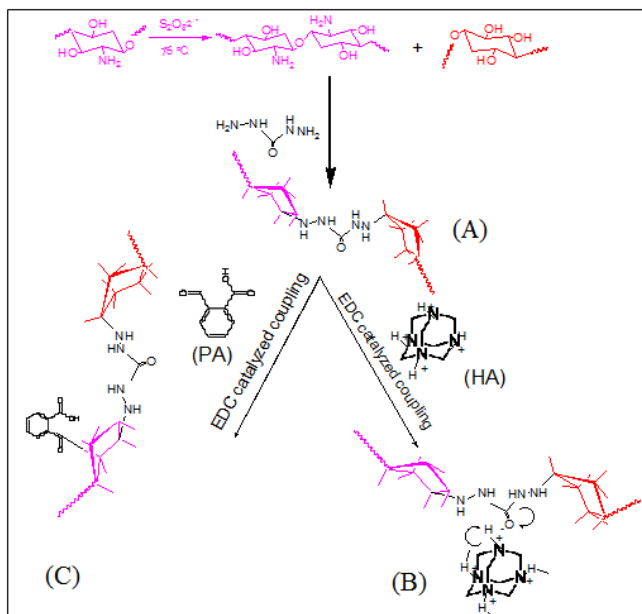


Figure 2. Synthetic route of native (A) nanohydrogel and their functionalization with hexamethylenetetramine (B), and phthalic-anhydride (C) for extended interaction with drug solution and cellular surfaces.

2.3. Significant properties of Hydrogel

The significant properties of hydrogel including swelling, porosity, crosslinking density and quality of solvent (water) can be fully understood by applying Flory–Rehner’s equation. Further, the porosity, number of pores, equilibrium swelling, equilibrium volume friction of hydrogel and average molecular weight of a chain between adjacent crosslinking points can be numerically calculated by using Flory–Rehner’s equation as shown in **Table 2**, respectively [20].

(a) Porosity.

The porosity of the hydrogel can be assessed by using Eq. 1 [21]

$$\text{Porosity\%} = \left[1 - \left\{ \frac{\rho_F}{\rho_P} \right\} \right] \times 100 \quad (\text{Eq. 1})$$

Where ρ_F is the density of polymeric phase (pure polymer). And ρ_P is the density of the hydrogel.

(b) Crosslinking density.

The hydrogel particles (ω_2) were allowed to swell in water until equilibrium to define the equilibrium swollen mass (ω_0). The mass of solvent fraction (ω_1) after swelling was calculated by Eq. 2 [21]

$$\omega_1 = \omega_0 - \omega_2 \quad (\text{Eq. 2})$$

The equilibrium volumetric swelling ratio (Q) was calculated by equation Eq. 3 [21]

$$Q = \frac{V_1 + V_2}{V_2} = \frac{\frac{\omega_1}{\rho_1} + \frac{\omega_2}{\rho_2}}{\frac{\omega_2}{\rho_2}} \quad (\text{Eq. 3})$$

Where V is volume, ω symbolize mass, ρ refers to density, subscript 1 stands for solvent while 2 for hydrogel. The swelling ratio can also be calculated from the graph using equation Eq. 4.

The equilibrium volume fraction of polymer in hydrogel ν_P is given by the Eq. 4

$$\nu_P = Q^{-1} \quad (\text{Eq. 4})$$

Flory-Rehner’s equation based on the equilibrium swelling of polymer in solvent for three dimensional networks was adopted. The Flory-Rehner’s equation is given as Eq. 5 [21]

$$-[\ln(1 - \nu_P) + \nu_P + \chi \nu_P^2] = N V_s [\nu_P^{1/3} - \frac{\nu_P}{2}] \quad (\text{Eq. 5})$$

Where N is the crosslinking density (mol/m^3), V_s is the molar volume of the solvent water, which are 18.3 ml/mol. Using 0.5 as the interaction parameter of χ .

The crosslinking density N and the average molecular weight of a chain between adjacent crosslinking points M_c were calculated by using Eq. 6 [22]

$$-[\ln(1 - \nu_P) + \nu_P + \chi \nu_P^2] = \frac{\rho_2}{M_c} V_s \nu_P^{1/3} \quad (\text{Eq. 6})$$

It should be pointed that ρ_2 was replaced with the experimentally measured density of each hydrogel, which was 0.45 g/cm^3 for medium molecular weight. The solvent (water) density is 1 g/cm^3 with molar volume of 18 cm^3/mol . The value χ for copolymerized chitosan was estimated as 0.5 accordingly [23]. Such numerical investigations have significant effects regarding physicochemical and drug administration aspects of chitosan built hydrogel for controlled drug delivery applications.

2.4. Solid state ^{13}C -NMR analysis

Solid state ^{13}C NMR spectra at 50.28 MHz were performed on a Bruker AMX-200 spectrometer equipped with an HP amplifier at 200.13 MHz and 120 W. In all measurements the spin rate was 8 KHz. In order to obtain the best signal-to-noise ratio of all C signals and to minimize artifacts, the proper contact time was carefully chosen according to a previously reported procedure. In order to avoid signals saturation a recycle time of 40 seconds and a ^{13}C pulse width of 3 μs corresponding to a flip angle of 60° were used [24, 25].

2.5. Field Emission Scanning Electron Microscopic (FESEM) Analysis.

FESEM is a widely used technique in order to define the specific ‘network’ arrangement in hydrogel. Scanning electron microscope was used to determine the morphology, porosity and composition of hydrogel particles and aggregates [26, 27]. The bright spots reflect small conductance of the hydrogel if the samples are scanned without coating for SEM analysis. The purified and dried gel samples were placed on an aluminum mount, sputtered with gold and palladium and then scanned at an accelerating voltage of 5.0 kV. SEM analysis was conducted at the School of Materials and Mineral Resources Engineering USM by using ZEISS Supra 35 VP model according to ASTM-E986 (2010). The images at 5 KX, 10 KX, 25 KX and 30 KX magnifications were captured.

2.6. Photoluminescence analysis of drug loading and release.

Bromocresol green with specific Absorbance of 423.25 nm was selected as model hydrophobic- anionic drugs to study the drug loading and release profile of native and functionalized hydrogel by using UV–vis spectrophotometer. Such a combination of model drugs selection is based on their potential application in term of investigating hydrophobic drug administration to a more than 40% of drugs are hydrophobic in nature which still need specific

hydrophilic ligands to counterbalance the amphiphilic balance at cellular surfaces.

A fixed amount of dried hydrogel was allowed to mix with an aqueous solution of the drug with pre-determined concentration. Drug loading and release profiles were obtained from the hydrogel in a shaker incubator at 75 rpm at 37 °C. 04 mL of each solution was analyzed for the drug concentration/ 20 min delay by using a UV- Vis spectrophotometer. An equal volume of the same solution medium was added back to maintain a constant volume. The drug release study was investigated in a sophisticated

dissolution apparatus by immersing 0.45 g of drug loaded dried hydrogel beads in 250 mL of pH 6.85 solutions. After mixing, the mixture was centrifuged at 75 rpm at 37 °C. 04 mL of the solution was taken for analysis with continuously replacing by fresh buffer solution to maintain a steady volume. Thus the concentration of the released drug was investigated in term of Absorbance followed by concentration differences. The in vitro release tests of all samples were conducted in triplicate at specified time intervals [28].

Table 1. Feed composition of A, B and C nanohydrogel.

| Sample Code | Chitosan (mg) | Alginate (mg) | CH (M) | SDS (mg) | APS (M) | B (mg) | C (mg) | EDC (mg) | Curing hours | Curing temp °C | Curing Dialysis |
|-------------|---------------|---------------|--------|----------|---------|--------|--------|----------|--------------|----------------|-----------------|
| A | 650 | 550 | 0.5 | 10 | 0.5 | - | - | - | 23.5 | 75 | 7 |
| B | 650 | 550 | 0.5 | 10 | 0.5 | 150 | - | 150 | 15 | 25 | 7 |
| C | 650 | 550 | 0.5 | 10 | 0.5 | - | 150 | 150 | 15 | 25 | 7 |

Table 2. Significant parameters of C1, C and C3 hydrogel.

| Hydrogel Code | Density (g/cm ³) | Porosity (%) | Polymer volume friction (v _p) | M _w of adjacent crosslink chain (M _c / kg.mol ⁻¹) | Crosslinking density (mol. m ³) |
|---------------|------------------------------|--------------|---|---|---|
| A | 2.14 | 60 | 0.042 | 3.13 | 25.17 |
| B | 2.35 | 68 | 0.031 | 3.44 | 20.31 |
| C | 2.17 | 71 | 0.035 | 3.51 | 19.47 |

3. RESULTS

3.1. Solid State Nuclear Magnetic Resonance (¹³C-NMR) Analysis.

In comparison to liquid- state ¹³C-NMR studies, the peaks in solid-state NMR spectra are very broad due to bulky group,anisotropic and orientation effects. Further, the intensity of peak lines are greatly affected due to low sensitivity and poor resolution as several peaks overlap each other at low resolution. The experimentally-determined solid state ¹³C NMR spectra of functionalized hydrogel samples coded as B and C are revealed in **Figure 3 (A,B and C)** respectively. The experimental peaks were compared with the reported literature. The desirable and characteristic peak for -C-NH₂ is observed at 35-45 ppm (a), representing amine functionality in chitosan, responsible for swelling and de-swelling for controlled- drug administration at physiological pH. The resonance peak-CH₂ 40-46 ppm (b) -C-OH 50-55 ppm (c), -C-N 80-85 (d), amides 175-185 ppm (e), carbonyl 190-200 ppm (f) could be attributed to the reaction between CS, SR and the chemical crosslinker carbohydride. The hydrogel functionalized with Hexamethylenetetramine (B), has been verified by shifting of peaks and appearance of additional peak for heterocyclic ring (combination of C-N,-CH₂, -N-C-N groups) in the range of 210-230 ppm. In case of hydrogel functionalized with pthaic-anhydride (C), the appearance of peak for aromatic stretching around 200 ppm and absence of heterocyclic ring (in comparison to (B) is a direct clue of the carbon resonance could be credited to the degree of crosslinking and induced hydrophilicity.

3.2. Scanning Electron Microscopic (SEM) Analysis.

The Field Emmission Scanning Electron Microscopy revealed the native and functionalized hydrogel with nanoporous architecture with highly developed internal surface area and lower diffusional resistance as shown in **Figure 4** respectively. The results also addressed that the cross-sectional of native and functional

hydrogel did not resemble the surface structure. The hydrogel revealed co-continuous open porous structure, which showed that the product used as a drug and also loaded with a drug for interactions to stop the development of various infected cells inside the body. Such surfaces reflect higher interest for a variety of interactions both cationic and anionic in all aspects. The brightness observed in the images reflects the conductance of the nanohydrogel material as the samples were analyzed without coating to confirm the conductivity. Thus, the successive functionalization modified the morphology, porosity, cross-linking density and the surface roughness of the hydrogel which is desirable for better understanding and drug administration at physiological conditions [29]. Such functional hydrogel with extreme swelling capabilities due to extended interfaces with drug and cellular surfaces could be applied as an efficient drug delivery tool.

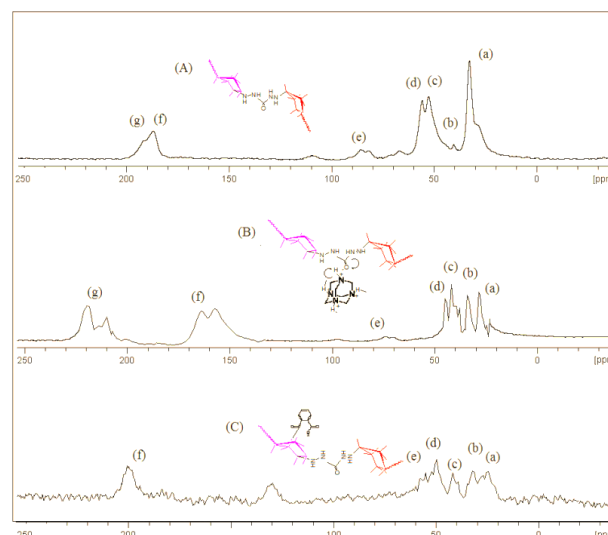


Figure 3. Solid state ¹³C NMR confirmation of native and functionalized Chitosan-co- Starch based nanohydrogel.

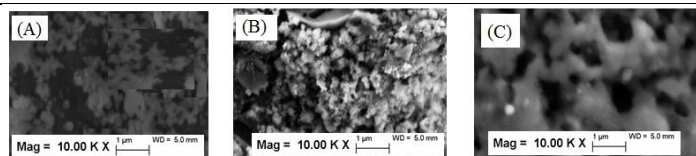


Figure 4. Field Emission Scanning electron microscopic (FESEM) analysis of native (A) and Functional (B and C) hydrogel dried at pH 7.45 and T= 25 °C.

3.3. Effect of pH.

A system responding to internal stimuli like pH has more significance as compared to external stimuli. The proposed system acts as multi-responsive to various stimuli including pH, temperature, ionic strength and urea respectively. Regarding pH effect, different pH exists in different parts of the body from saliva to extracellular tumor cells as blood (pH \approx 7.4-7.6), intracellular tumor (pH \approx 6.4-7.2), colon (pH \approx 7.0-7.5), duodenum (pH \approx 6.4-8.2) as per reported literature. Thus, the development of hydrogel is challenging for targeted and effective drug administration at specific pH without any side effect. One such system, aims to target the blood and intracellular pH is proposed which effectively work in the pH range of 6.0-7.50.

The presence of specific groups either acidic/ anionic (carbonyl, carboxylic, sulphonic, carbonyl) or basic/ cationic (ammonium, amino) in the hydrogel matrices have the potential to donate or accept the protons in aqueous medium at specific pH [20]. Such pendent groups suffer from electrostatic repulsion followed by conformational modifications in response to the pH causing the hydrogel to swell and thus release the loaded drug at targeted site. Further, the stability in term of zeta potential from -10 mV were observed at lower pH as compared to 26 mV at physiological pH (**Figure 5**). This reflects the biocompatible nature of the proposed system where highly interacting cationic groups are dominant in the pH range \approx 6.0- 7.45. Hence, at physiological conditions and at tumor site the hydrogel with the active functionalities have been identified with cationic and specified pH. This happens due to ions- counter-ions balance in addition to the protonated cationic groups present in chitosan per segment. At lower pH, the hydrogel network is not yet protonated so present in shrunken state, but as the value increases to pH \approx 6.5, which is comparable to Chitosan pK_a value, (pK_a \approx 6.54), the NH₂ groups in chitosan per segment get protonated in aqueous solution and thus several NH₃⁺ groups of chitosan appear and suffer electrostatic repulsion, moving far apart from each other, absorbing enormous amounts of water to swell with an increased hydrodynamic diameter. A higher degree of ionization is required for higher swelling to release the entrapped drug/ bioactive species. So the art of release and controlled release of the drugs, dyes or proteins by the hydrogel network is hidden in the interacting groups, specified pK_a values and specified pH of the system [30, 31]. For the efficient hydrogel, highly reactive groups with extreme ionic mobilities, positive zeta potential and conductivities are required for prolonged and efficient drug delivery at the targeted site as determined for the proposed system which may be applied as a potential candidate for the described theme.

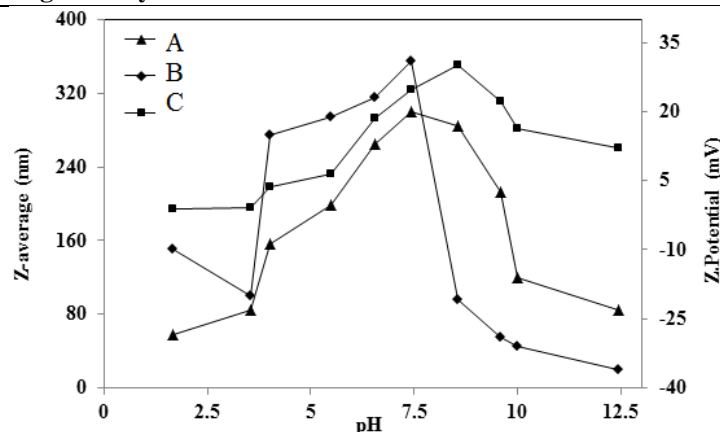


Figure 5. Physicochemical (swelling) performance of native and functionalized hydrogel as a function of pH (1.68-12.45) at 37 °C.

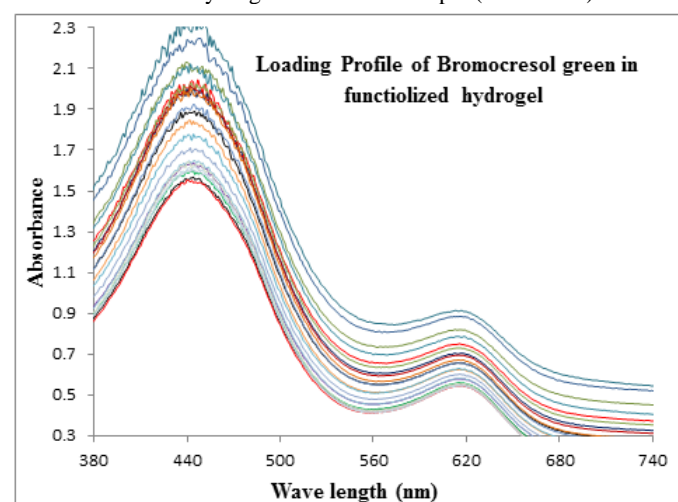


Figure 6. Representative profile of model- drug loading in chitosan built hydrogel functionalized with phthalic anhydride in term of decrease in absorbance as a function of time.

3.4. Thermo-kinetic of model drug loading.

A representative profile for the time dependent model drug loading (after 20 minutes delay) in chitosan built hydrogel (B) is shown in **Figure 6**. The experimental absorbance obtained at 446 nm wavelength reflect the standard absorbance of Bromocresol green which is in decreasing order due to decrease in concentration of the dye after effectively loading as a function of time ranging from 20-740 minutes. The stability and uniformity in wavelength revealed the fact that structure of model drug was not affected during loading and was physically entrapped in hydrogel matrices. The drug loading up to 75.94 % and controlled release up to 85.56% was investigated to explore the effect of surface modification, affecting the drug loading and release profiles of hydrophobic drugs at physiological conditions. To explore the effect of temperature, the drug administration was performed at different temperature ranging from 298-348 K and rate constant at each temperature was determined by applying Arrhenius and Eyring's equation respectively. For *in vitro* drug administration such investigations could be applied as standard values as performed for the first time to explore the thermodynamic of drug administration for controlled drug delivery. The selection of model drug (Bromocresol green) also reflects the hydrogel action to perform *in vivo* at cellular level, making the hydrogel to be applied practically [1, 19]. As shown in **Figure 7**, a linear trend was observed in the reaction (interaction of drug with hydrogel) as a function of temperature. The first order kinetic was applied in

each case to investigate the reaction rate constant abbreviated as (k_{app}) with the correlation coefficient (R^2) ranging 0.96-0.98. An increase in the corresponding interaction between hydrogel and drug administration was observed which may be attributed to the increase in collision frequency and extended interactions between hydrogel and model drug at higher temperatures. All The thermodynamic and thermokinetic parameters were calculated by plotting $\ln(k_{app})$ and $\ln(k_{app}/T)$ as a function of inverse of temperature respectively. The results concluded that drug loading and release in aqueous medium at specific pH was a spontaneous process, without any real bond formation as verified from lower values of enthalpy. Also, the positive values for entropy expressed a higher degree of freedom and non-stop interaction of model drug with hydrogel at specified conditions. The calculated parameters to reflect the spontaneous and physical entrapment of drug loading in hydrogel matrices are shown in **Table 3**.

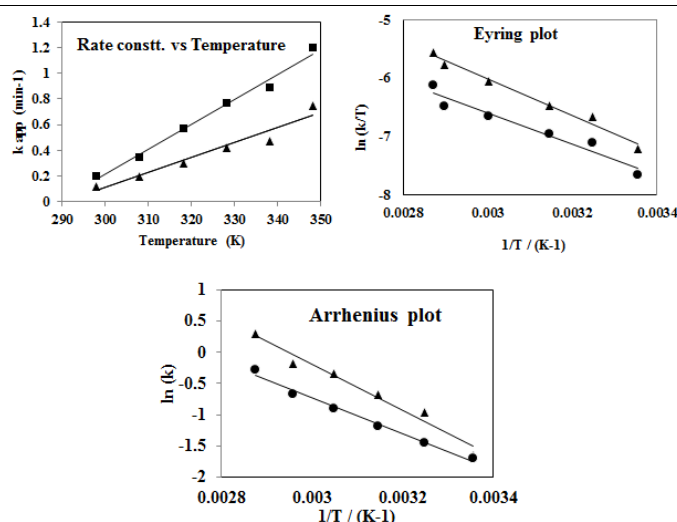


Figure 7. Representative plots of rate constant (k_{app}), thermokinetic and thermodynamic parameters as a function of temperature by applying Eyring equation ($\ln(k_{app}/T)$ vs $1/T$), and Arrhenius equation ($\ln(k_{app})$ vs $1/T$) in chitosan built hydrogel.

Table 3. The activation parameters for the model drugs in chitosan built hydrogel.

| Drug | ΔH^* (kJ/mol) | ΔS^* (kJ/mol.K) | E_a^* (kJ/mol) |
|------|-----------------------|-------------------------|------------------|
| A | 23.14 | 50.24 | 22.4 |
| B | 20.48 | 55.13 | 18.20 |
| C | 18.48 | 41.95 | 20.87 |

4. CONCLUSIONS

CS-co-SR hydrogel was successfully synthesized and were functionalized with phthalic-anhydride and hexamethylenetetramine via EDC catalyzed carbodiimide coupling respectively. With the successive functionalization the significant properties like porosity increases (from 60-71%), and corresponding decrease in crosslinking density (from 25.17- 19.47 mol.m³) were calculated and were attributed to the formation of hydrophilic contacts with aqueous solution. The FESEM analysis revealed C in form of uniform particle size, porosity and deep pores with high internal surface area for extreme swelling and interacting with the drug and biomolecules for efficient drug administration. The

physicochemical properties with (z-average \approx 75-350 nm), polydispersity index (PDI \approx 0.50-0.61) were observed by using laser light scattering. With the successive functionalization, the drug release was increased from 65- 81% respectively due to development of extended interfaces of functional moieties with drug solution and cellular surface.

The physicochemical and electrokinetic performances suggested the selective hydrogel as promising carriers for the anionic drugs, as the release profile can be tuned and sustained with such biocompatible moieties.

5. REFERENCES

- Ullah, F.; Javed, F.; Othman, M.B.H.; Khan, A.; Gul, R.; Ahmad, Z.; Md Akil, H. Synthesis and functionalization of chitosan built hydrogel with induced hydrophilicity for extended release of sparingly soluble drugs. *Journal of Biomaterials Science, Polymer Edition* **2018**, 29, 376-396, <https://doi.org/10.1080/09205063.2017.1421347>.
- Gaware, S.A.; Rokade, K.A.; Kale, S.N. Silica-chitosan nanocomposite mediated pH-sensitive drug delivery. *Journal of Drug Delivery Science and Technology* **2019**, 49, 345-351, <https://doi.org/10.1016/j.jddst.2018.11.022>.
- Ullah, F.; Othman, M.B.H.; Javed, F.; Ahmad, Z.; Akil, H.M. Classification, processing and application of hydrogels: A review. *Materials Science and Engineering: C* **2015**, 57, 414-433, <https://doi.org/10.1016/j.msec.2015.07.053>.
- Caccavo, D. An overview on the mathematical modeling of hydrogels' behavior for drug delivery systems. *International Journal of Pharmaceutics* **2019**, 560, 175-190, <https://doi.org/10.1016/j.ijpharm.2019.01.076>.
- Martínez-Martínez, M.; Berna, G.R.; Bermejo, M.; Alvarez, I.G.; Alvarez, M.G.; Merino, V. Covalently crosslinked organophosphorous derivatives-chitosan hydrogel as a drug

- delivery system for oral administration of camptothecin. *European Journal of Pharmaceutics and Biopharmaceutics* **2019**, 136, <https://doi.org/10.1016/j.ejpb.2019.01.009>.
- Tan, H.; Jin, D.; Qu, X.; Liu, H.; Chen, X.; Yin, M.; Liu, C. A PEG-Lysozyme hydrogel harvests multiple functions as a fit-to-shape tissue sealant for internal-use of body. *Biomaterials* **2019**, 192, 392-404, <https://doi.org/10.1016/j.biomaterials.2018.10.047>.
- Xu, J.; Strandman, S.; Zhu, J.X.X.; Barralet, J.; Cerruti, M. Genipin-crosslinked catechol-chitosan mucoadhesive hydrogels for buccal drug delivery. *Biomaterials* **2015**, 37, 395-404, <https://doi.org/10.1016/j.biomaterials.2014.10.024>.
- Gorgieva, S.; Kokol, V. Preparation, characterization, and in vitro enzymatic degradation of chitosan-gelatine hydrogel scaffolds as potential biomaterials. *Journal of Biomedical Materials Research Part A* **2012**, 100, 1655-1667, <https://doi.org/10.1002/jbm.a.34106>.
- Delmar, K.; Bianco-Peled, H. Composite chitosan hydrogels for extended release of hydrophobic drugs. *Carbohydrate Polymers* **2016**, 136, 570-580, <https://doi.org/10.1016/j.carbpol.2015.09.072>.

10. Alison, L.; Demirörs, A.F.; Tervoort, E.; Teleki, A.; Vermant, J.; Studart, A.R. Emulsions stabilized by chitosan-modified silica nanoparticles: pH control of structure–property relations. *Langmuir* **2018**, *34*(21), 6147–6160, <https://doi.org/10.1021/acs.langmuir.8b00622>
11. Gohi, B.F.C.A.; Zeng, H.Y.; Pan, A.D.; Han, J.; Yuan, J. pH dependence of chitosan enzymolysis. *Polymers* **2017**, *9*(5), 1–20, <https://doi.org/10.3390/polym9050174>.
12. Kar, M.; Chourasiya, Y.; Maheshwari, R.; Tekade, R.K. Current developments in excipient Science: Implication of quantitative selection of each excipient in product development. In *Basic Fundamentals of Drug Delivery* **2019**, 29–83, <https://doi.org/10.1016/B978-0-12-817909-3.00002-9>.
13. Merlot, A.M.; Kalinowski, D.S.; Kovacevic, Z.; Jansson, P.J.; Sahni, S.; Huang, M.L.H.; Lane, D.J.R.; Lo, H.; Richardson, D.R. Exploiting cancer metal metabolism using anti-cancer metal-binding agents. *Current Medicinal Chemistry* **2019**, *26*(2), 302–322, <https://doi.org/10.2174/0929867324666170705120809>.
14. Hennink, W.; Van Nostrum, C.F. Novel crosslinking methods to design hydrogels. *Advanced Drug Delivery Reviews* **2012**, *64*, 223–236, [https://doi.org/10.1016/S0169-409X\(01\)00240-X](https://doi.org/10.1016/S0169-409X(01)00240-X).
15. George, M.; Abraham, T.E. Polyionic hydrocolloids for the intestinal delivery of protein drugs: alginate and chitosan—a review. *Journal of Controlled Release* **2006**, *114*, 1–14, <https://doi.org/10.1016/j.jconrel.2006.04.017>.
16. Wang, Q.; Zhang, J.; Wang, A. Preparation and characterization of a novel pH-sensitive chitosan-g-poly (acrylic acid)/attapulgit/sodium alginate composite hydrogel bead for controlled release of diclofenac sodium. *Carbohydrate polymers* **2009**, *78*, 731–737, <https://doi.org/10.1016/j.carbpol.2009.06.010>.
17. Rasib, S.Z.M.; Akil, H.M.; Khan, A.; Hamid, Z.A.A. Controlled release studies through chitosan-based hydrogel synthesized at different polymerization stages. *International Journal of Biological Macromolecules* **2019**, *128*, 531–536, <https://doi.org/10.1016/j.ijbiomac.2019.01.190>.
18. Chi, H.; Qiao, Y.; Wang, B.; Hou, Y.; Li, Q.; Li, K.; Liu, Z. Swelling, thermal stability, antibacterial properties enhancement on composite hydrogel synthesized by chitosan-acrylic acid and ZnO nanowires. *Polymer-Plastics Technology and Materials* **2019**, 1–13, <https://doi.org/10.1080/25740881.2018.1563138>.
19. Ullah, F.; Othman, M.B.H.; Javed, F.; Ahmad, Z.; Akil, H.M.; Rasib, S.Z.M.R. Functional properties of chitosan built nanohydrogel with enhanced glucose-sensitivity. *International journal of Biological Macromolecules* **2016**, *83*, 376–384, <https://doi.org/10.1016/j.ijbiomac.2015.11.040>.
20. Elliott, J.E.; Macdonald, M.; Nie, J.; Bowman, C.N. Structure and swelling of poly (acrylic acid) hydrogels: effect of pH, ionic strength, and dilution on the crosslinked polymer structure. *Polymer* **2004**, *45*, 1503–1510, <https://doi.org/10.1016/j.polymer.2003.12.040>.
21. Flory, P.J. *Principles of polymer chemistry*. Cornell University Press, 1953.
22. Xia, Z.; Patchan, M.; Maranchi, J.; Elisseeff, J.; Trexler, M. Determination of crosslinking density of hydrogels prepared from microcrystalline cellulose. *Journal of Applied Polymer Science* **2013**, *127*, 4537–4541, <https://doi.org/10.1002/app.38052>.
23. Baier, L.J.; Bivens, K.A.; Patrick, C.W.Jr.; Schmidt, C.E. Photocrosslinked hyaluronic acid hydrogels: natural, biodegradable tissue engineering scaffolds. *Biotechnology and Bioengineering* **2003**, *82*, 578–589, <https://doi.org/10.1002/bit.10605>.
24. Dorkoosh, F.; Brussee, J.; Borchard, G.; Rafiee-Tehrani, M.; Junginer, H.E. Preparation and NMR characterization of superporous hydrogels (SPH) and SPH composites. *Polymer* **2000**, *41*, 8213–8220, [https://doi.org/10.1016/S0032-3861\(00\)00200-7](https://doi.org/10.1016/S0032-3861(00)00200-7).
25. Ullah, F.; Javed, F.; Othman, M.B.H.; Ahmad, Z.; Akil, H.M. Synthesis and physicochemical investigation of chitosan-built hydrogel with induced glucose sensitivity. *International Journal of Polymeric Materials and Polymeric Biomaterials* **2017**, *66*, 824–834, <https://doi.org/10.1080/00914037.2016.1276061>.
26. Yadollahi, M.; Farhoudian, S.; Namazi, H. One-pot synthesis of antibacterial chitosan/silver bio-nanocomposite hydrogel beads as drug delivery systems. *International Journal of Biological Macromolecules* **2015**, *79*, 37–43, <https://doi.org/10.1016/j.ijbiomac.2015.04.032>.
27. Kajari, P.B.; Manjeshwar, L.S.; Aminabhavi, T.M. Novel blend microspheres of poly (vinyl alcohol) and succinyl chitosan for controlled release of nifedipine. *Polymer bulletin* **2013**, *70*, 3387–3406, <https://doi.org/10.1007/s00289-013-1029-6>.
28. Rasib, S.Z.M.; Akil, H.M.; Khan, A.; Hamid, Z.A.A. Controlled release studies through chitosan-based hydrogel synthesized at different polymerization stages. *International Journal of Biological Macromolecules* **2019**, *128*, <https://doi.org/10.1016/j.ijbiomac.2019.01.190>.
29. Jagur-Grodzinski, J. Polymeric gels and hydrogels for biomedical and pharmaceutical applications. *Polymers for Advanced Technologies* **2010**, *21*, 27–47, <https://doi.org/10.1002/pat.1504>.
30. Liutkevičius, A.; Speiciene, V.; Alencikiene, G.; Sekmokiene. Influence of chitosan on microbiological data and quality characteristics of spreadable curd cheese and mayonnaise. *Veterinarija ir Zootechnika* **2015**, *69*, 38–47, <https://doi.org/10.3390/polym9050174>.
31. Zhang, Y.; Tao, L.; Wei, Y. Synthesis of multiresponsive and dynamic chitosan-based hydrogels for controlled release of bioactive molecules. *Biomacromolecules* **2011**, *12*, 2894–2901, <https://doi.org/10.1021/bm200423f>.

6. ACKNOWLEDGEMENTS

This research is supported by the School of Material and Mineral Source Engineering, Universiti Sains Malaysia under the project Grant FRGS-203/PBAHAN-6071337.



© 2019 by the authors. This article is an open access article distributed under the terms and conditions of the Creative Commons Attribution (CC BY) license (<http://creativecommons.org/licenses/by/4.0/>).